PNAS RESEARCH ARTICLE | ECOLOGY
BIOPHYSICS AND COMPUTATIONAL BIOLOGY OPEN ACCESS

Prey can detect predators via electroreception in air

Sam J. England[a,b,1] and Daniel Robert[a]

Edited by John Hildebrand, The University of Arizona, Tucson, AZ; received January 12, 2024; accepted April 23, 2024

Predators and prey benefit from detecting sensory cues of each other's presence. As they move through their environment, terrestrial animals accumulate electrostatic charge. Because electric charges exert forces at a distance, a prey animal could conceivably sense electrical forces to detect an approaching predator. Here, we report such a case of a terrestrial animal detecting its predators by electroreception. We show that predatory wasps are charged, thus emit electric fields, and that caterpillars respond to such fields with defensive behaviors. Furthermore, the mechanosensory setae of caterpillars are deflected by these electrostatic forces and are tuned to the wingbeat frequency of their insect predators. This ability unveils a dimension of the sensory interactions between prey and predators and is likely widespread among terrestrial animals.

sensory ecology | predator–prey interactions | caterpillars | wasps | electrostatics

Significance

Our study reveals the finding that some terrestrial animals can detect the electric field emanating from their electrostatically charged predators and use this sense to initiate defensive behaviors. By reporting electroreception in terrestrial predator–prey interactions, our study stands to significantly advance our understanding of animal sensory systems and predator–prey dynamics. Furthermore, we demonstrate that the mechanosensory hairs of caterpillars exhibit an electromechanical resonance to the wingbeat frequency of flying predatory insects, which points to this electrical ecological interaction applying a selection pressure, resulting in the evolution of tuned electroreceptive systems. Therefore, our finding provides direct evidence for a driver of evolution by natural selection: ecologically relevant static electricity.

Predator–prey interactions are literally a matter of life and death. As such, they are one of the most potent and ubiquitous ecological drivers of evolution by natural selection among animals (1–3). Prey and predators alike therefore benefit from sensory intelligence to detect and locate each other's presence in space and time, and thus evolutionary arms races develop between them to exploit better or entirely novel sensory cues.

Electrically charged objects emit electric fields that exert forces on other charged objects (4). Because animals and plants are nearly always electrically charged, these electrical forces permeate the natural environment (5, 6). Yet, the potential ecological role of these electric fields and forces has historically gone largely unnoticed (5). To rectify this, we investigated whether naturally occurring static electricity provides a hidden dimension to predator–prey interactions, as a source of sensory information. As it has previously been shown that many flying insect species accumulate electrostatic charge (5, 7–12), we predicted that flying predatory insects perturbate the ambient electric field in their vicinity. If detectable, these alterations in electric field could provide prey with information on the presence and location of their predators, constituting a sensory cue. Here, we hypothesize that this form of electroreception enables prey species to detect predators using electrostatic fields, transforming our understanding of predator–prey dynamics and ecology.

Addressing this hypothesis, behavioral, biophysical, morphological, and computational techniques were deployed on three species of lepidopteran caterpillar, namely the cinnabar moth (*Tyria jacobaeae*) (Fig. 1*A*), scarce vapourer moth (*Telochurus recens*) (Fig. 1*B*), and European peacock butterfly (*Aglais io*) (Fig. 1*C*), as well as the predatory common wasp (*Vespula vulgaris*) (Fig. 1*D*).

Results

The electric field produced by a typical predator of caterpillars first needed to be characterized. To do so, an electrostatic charge sensor was mounted at the entrance of a common wasp nest. Wasps would fly freely through this sensor, upon which their net electrostatic charge could be measured [in picoCoulombs (pC), methodology fully described in *Materials and Methods*]. These noncontact measurements confirm that predatory wasps carry a nonnegligible electrostatic charge (mean ± SD = 8.81 ± 12.81 pC, n = 612) (Fig. 2*A*), at magnitudes similar to the charges measured on other terrestrial fauna (5). As such, wasps are sources of electric field potentially detectable by electroreceptive prey.

Similarly, using the same electrostatic charge sensor, the net charge of each caterpillar species situated on their foodplants was measured by dropping them through the sensor. This showed that caterpillars are not highly charged in comparison to other animals of their size (*T. jacobaeae* mean ± SD = 0.48 ± 1.15 pC, n = 28; *T. recens* mean ± SD = 1.64 ± 1.23 pC, n = 38; *A. io* mean ± SD = −1.67 ± 7.05 pC, n = 44) (Fig. 2*A*) (5).

These mean charge values for predator and prey were then used to inform a computational three-dimensional finite element analysis to quantify the strength of electric field generated by a wasp approaching a caterpillar situated on a plant. This model suggests

Author affiliations: [a]School of Biological Sciences, Faculty of Life Sciences, University of Bristol, Bristol BS8 1TQ, United Kingdom; and [b]Department of Evolutionary Morphology, Museum für Naturkunde–Leibniz Institute for Evolution and Biodiversity Science, Berlin 10115, Germany

Author contributions: S.J.E. and D.R. designed research; S.J.E. performed research; S.J.E. contributed new reagents/analytic tools; S.J.E. analyzed data; and S.J.E. and D.R. wrote the paper.

The authors declare no competing interest.

This article is a PNAS Direct Submission.

[1]To whom correspondence may be addressed. Email: sam.england@bristol.ac.uk or sam.england@mfn.berlin.

This article contains supporting information online at https://www.pnas.org/lookup/suppl/doi:10.1073/pnas.2322674121/-/DCSupplemental.

Published May 20, 2024.

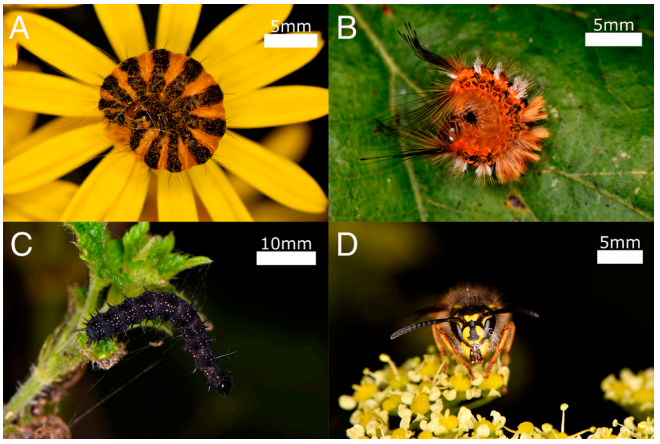

Fig. 1. Photographs of the four species investigated in this study. (*A*) The caterpillar of the cinnabar moth (*T. jacobaeae*) assuming a defensive coiling posture. (*B*) The caterpillar of the scarce vapourer moth (*T. recens*) assuming a defensive coiling posture. (*C*) The caterpillar of the European peacock butterfly (*A. io*), midway through a defensive flailing motion. (*D*) The predatory common wasp (*V. vulgaris*).

that at a distance of a few centimeters, the electric field between a wasp and caterpillar is on the order of kilovolts per meter (Fig. 2*B*).

This calculated electric field strength was in turn used to inform the stimulus presented to the caterpillars in behavioral experiments. For all caterpillars, electric stimuli were presented that mimicked the electric field emanating from a common wasp intermittently flying nearby, modulated by its 180 Hz wingbeat frequency (13, 14). This modulation exists because the wings are charged, and as they flap, oscillating closer and further from the prey, the electric field strength will increase when the wings are closer, and decrease when the wings are further, creating an oscillation in the electric field (15). Stimuli consisted of 2-s bursts of 180 Hz sinusoidal electric field at ecologically relevant magnitudes, followed by 2 s of electrical silence; a regime repeated until the end of each trial. Control trials involved identical experimental configurations and protocols but with the electrodes disconnected from the voltage source. Different behavioral assays were developed for each caterpillar species to best accommodate their varying behavioral repertoires. *T. jacobaeae* and *T. recens* caterpillars were exposed to the electrical stimulus after inducing a defensive coiling action (as seen in Fig. 1 *A* and *B*) by grasping them in soft entomological forceps for 20 s, and then placing them directly underneath a spherical electrode emitting the stimulus (Fig. 3 *A*, *Left*). The time taken for each caterpillar to both uncoil and subsequently commence walking was then recorded.

T. jacobaeae caterpillars remained coiled for significantly longer (U = 71.5, $P = 0.02$, treatment n = 17, control n = 16) and took longer to commence walking (U = 33, $P = 8 \times 10^{-5}$) after a simulated attack when the electric field was on, compared to control trials (Fig. 3 *C* and *D*). Likewise, *T. recens* caterpillars also took significantly longer to uncoil (U = 87, $P = 0.03$, treatment n = 18, control n = 17) after a simulated attack when the electric field was on, compared to control trials (Fig. 3*B*). Because *A. io* caterpillars do not exhibit the same defensive coiling behavior, defensive flailing and biting behaviors (Fig. 1*C*) were examined instead. *A. io* caterpillars were exposed to the electrical stimulus as they freely passed between parallel electrode plates, while climbing and descending a vertical pole (Fig. 3 *A*, *Right*). In this experimental paradigm, *A. io* caterpillars spent significantly more time flailing (U = 20, $P = 0.01$, treatment n = 11, control n = 10) (Fig. 3*E*), and were observed biting the electrodes exclusively, only when the electric field was switched on (U = 25, $P = 0.009$, treatment n = 11, control n = 10) (Fig. 3*F*). All of the behaviors witnessed are well characterized defensive strategies of caterpillars (16), and therefore these data strongly indicate that the caterpillars are capable of detecting the electric fields emitted by their predators, and perceive them as a threat.

To elucidate the mechanism of electroreception in caterpillars, their anatomies were examined for potential electroreceptive structures under scanning electron microscopy (SEM). Several candidate structures were identified across the three species, namely various filiform setae, many of which appear to be articulated at the base and thus are likely to be mechanoreceptive (Fig. 4). Histology, microcomputed tomography, or electrophysiology are needed to definitively confirm this. These filiform setae are present in many species of caterpillars and have been shown to sense particle-velocity sounds at the wingbeat frequencies of predators or parasitoids, which like the electric fields shown here, induce defensive behaviors (17–25). Therefore, if these setae can also be actuated by electric fields, they are well poised to act as electroreceptors too.

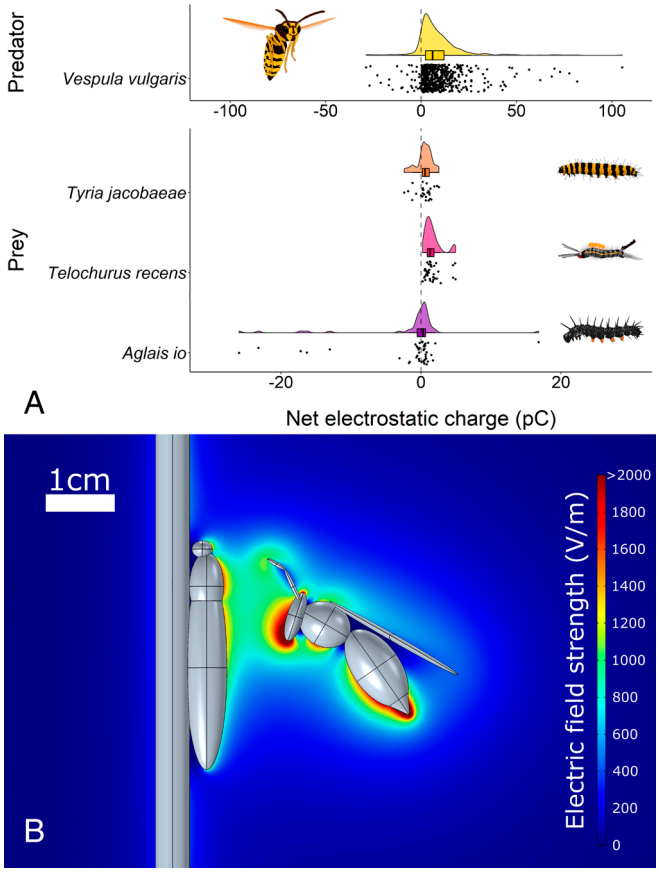

Fig. 2. Characterization of the physical electrical forces acting between predatory wasps and prey caterpillars. (*A*) Measurements of the net electrostatic charge carried by a predatory wasp, *V. vulgaris* (yellow), and three species of prey caterpillar, *T. jacobaeae* (orange), *T. recens* (pink), and *A. io* (purple). The dashed line denotes transition from negative to positive charge values. Half violins show distribution of data. Note different scales between wasps and caterpillars. (*B*) Two-dimensional slice through the center of a three-dimensional computational model of the electric field strength between a wasp and a caterpillar situated on the stem of a plant. The wasp was assigned a charge of +10 pC, based on the mean charge measured for *V. vulgaris*, and the caterpillar assigned a charge of −2 pC, based on the mean charge measured for *A. io*. The plant was defined as electrically grounded (5, 12–16). Electrical material properties were based on values from the literature (*SI Appendix*, Table S2). Electric field strength is denoted by color with values truncated above 2 kV/m for clarity. The 3D geometry of organisms is shown as gray.

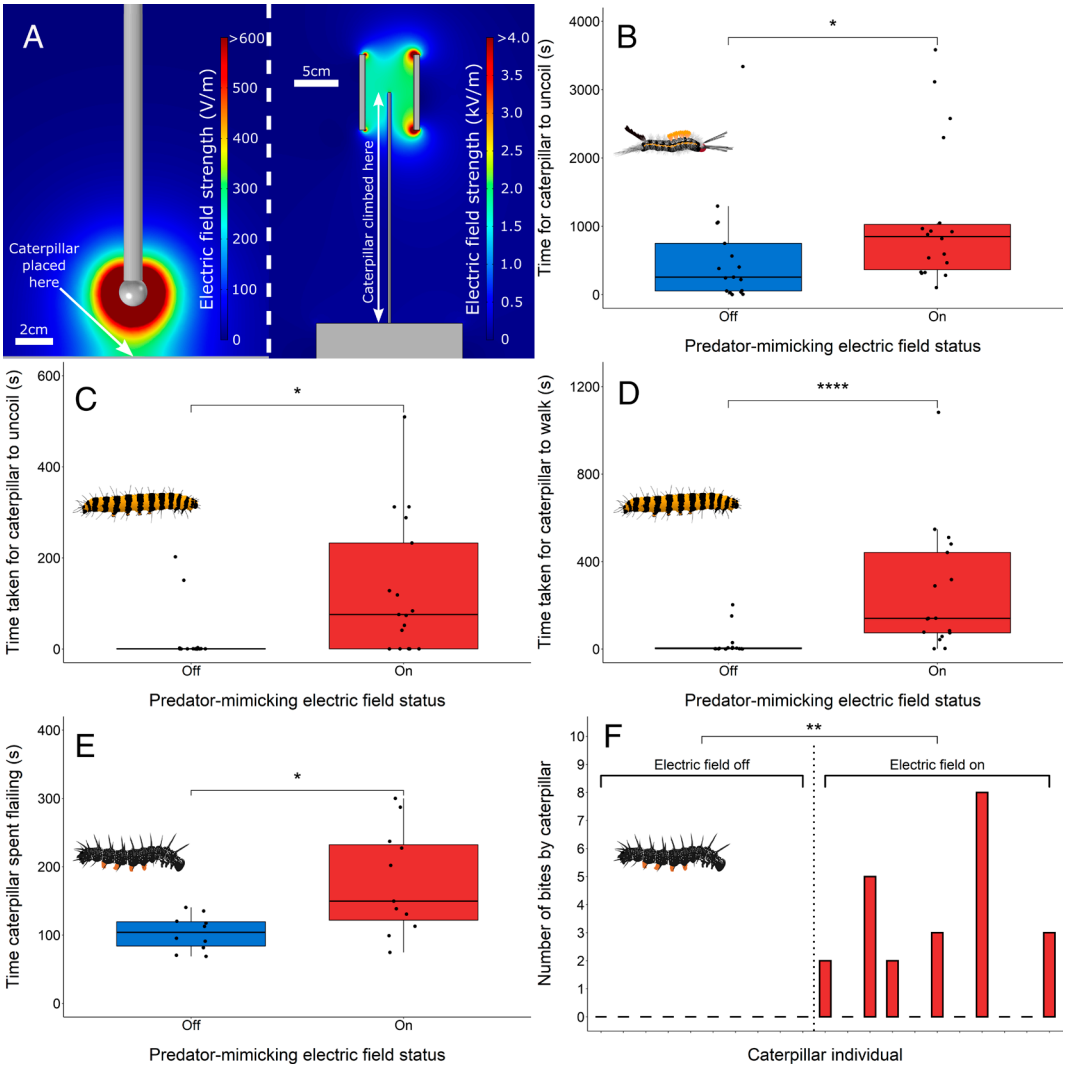

Fig 3. Behavioral apparatuses including their electric field strengths, and behavioral data. (*A*) Three-dimensional computational finite element analysis models showing the electric field strengths produced by the behavioral experimental apparatuses used for *T. jacobaeae* and *T. recens* (*Left*) and *A. io* (*Right*) at peak voltage. Color indicates electric field strength. Electric field strength values are graphically truncated above 600 V/m and 4 kV/m respectively for clarity. Gray surfaces show 3D geometry. (*B*) The time taken for *T. recens* caterpillars to uncoil after a simulated attack when exposed to a predator-mimicking electric field (red, *Right*) or not (blue, *Left*). (*C*) The time taken for *T. jacobaeae* caterpillars to uncoil after a simulated attack when exposed to a predator-mimicking electric field (red, *Right*) or not (blue, *Left*). (*D*) The time taken for *T. jacobaeae* caterpillars to commence walking after a simulated attack when exposed to a predator-mimicking electric field (red, *Right*) or not (blue, *Left*). (*E*) The time spent flailing by *A. io* caterpillars when exposed to a predator-mimicking electric field (red, *Right*) or not (blue, *Left*). (*F*) The number of biting bouts on the electrode enacted by *A. io* caterpillars when exposed to a predator-mimicking electric field (red, *Right*) or not (blue, *Left*). Asterisks indicate statistical significance from Mann–Whitney *U* test derived *P*-values: **P* < 0.05, ***P* < 0.01, ****P* < 0.001, *****P* < 0.0001.

To test this, the electromechanical responses of setae were examined for live *T. jacobaeae* and *T. recens* caterpillars using microscanning laser Doppler vibrometry (LDV). The vibrational responses of selected setae were measured in response to a range of electrical stimuli. All setae examined exhibited a mechanical response when exposed to an electric field oscillating at a frequency of 180 Hz (Fig. 5*A*), however, this response was strongest among the S1, S2, and S3 setae. Interestingly, maximal response occurred not at the driving frequency of 180 Hz, but at the second harmonic of the driving frequency, 360 Hz (Fig. 5 *B* and *C*). Such a response reveals that the dominant force acting on the setae is due to the external electric field polarizing the setae. This is distinct from relying upon a static charge on the surface of the setae, as documented in bees (5, 26, 27). Stimulation across a range of frequencies, using sweeps as analytical signals, reveals an electromechanical resonance of the setae across a frequency band of approximately 100 to 700 Hz (Fig. 5*D*), which translates to 50 to 350 Hz at the first harmonic. This resonance corresponds with the range of most insect wingbeat frequencies (28–30). The mean response of the setae peaks at 440.6 Hz, translating to 220.3 Hz at the first harmonic, which is in the region of a very typical wingbeat frequency for insects, including wasps, that predate upon caterpillars. Altogether, these data suggest that these setae are electromechanically sensitive and tuned to the wingbeat frequencies of their invertebrate predators.

Discussion

Our data show that all three species of caterpillar tested can detect the electric fields emitted by the predatory wasps that hunt them. Their behavioral responses to these electric fields demonstrate that an electrical stimulus alone is sufficient to elicit a defensive response, and therefore static electricity is likely a reliable cue used by caterpillars for predator detection. Before this study, electroreception has never been observed in a terrestrial predator–prey interaction, with all previous examples restricted to the aquatic environment (5, 31–35). This finding therefore introduces a dimension to predator–prey interactions on land prime for further investigation.

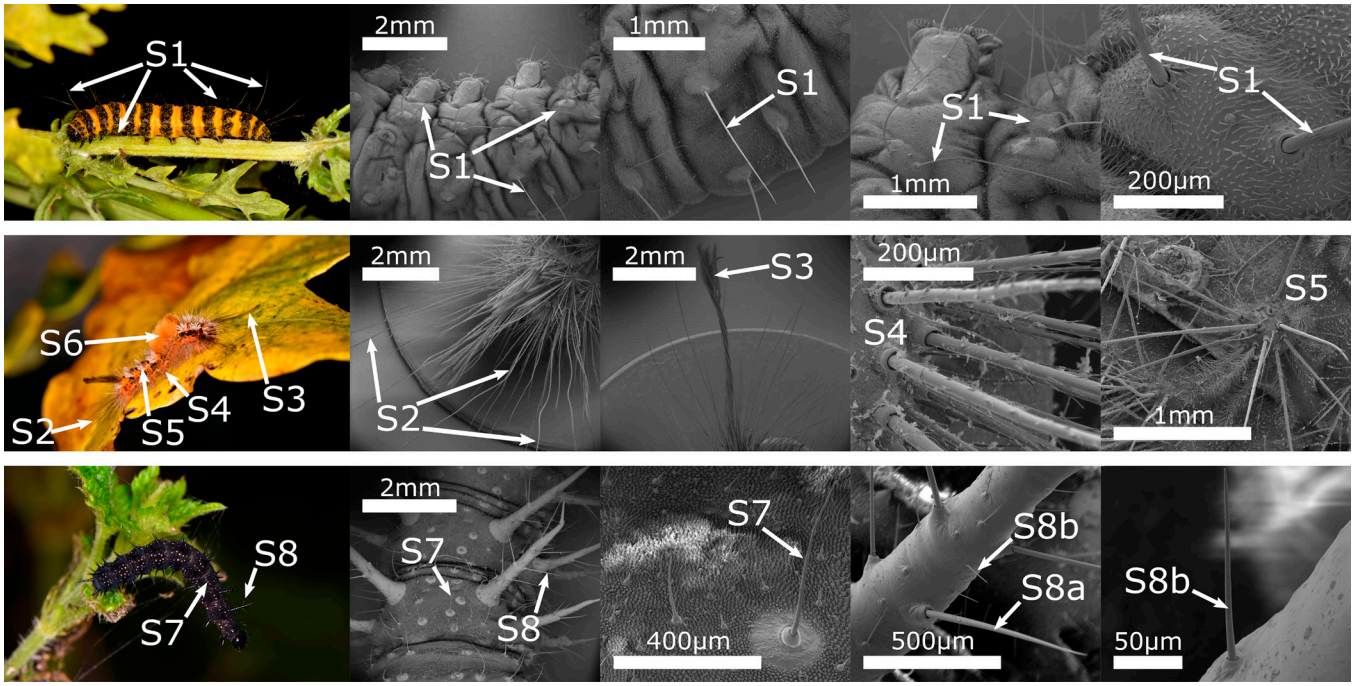

Fig. 4. Identification of setae (S1 to S8) as candidate electrosensory structures. SEM images of various candidate electrosensory structures examined for *T. jacobaeae* (*Top*), *T. recens* (*Middle*), and *A. io* (*Bottom*), alongside macrophotographs showing example locations of each on the caterpillar body. Numbers indicate seta types considered as distinct for the purposes of this study and are not exhaustively labeled.

Previous phylogenomic analyses suggest that the lineages of the three caterpillar species tested here evolutionarily diverged approximately 100 Mya, in the mid-cretaceous (36). This phylogenetic spread, alongside the ubiquity of setae and diversity of defensive behavioral responses to predators' electric fields observed in this study, may indicate that detection of predators by electrical means is a widespread ability among lepidopteran caterpillars. This possibility is further supported by the fact that the ability to detect ecologically relevant electric fields in air, aerial electroreception, is a known sensory modality in several other arthropod species. Aerial electroreception can be used by bumblebees (*Bombus terrestris*) and hoverflies (*Eristalis tenax* and *Cheilosia albipila*) to

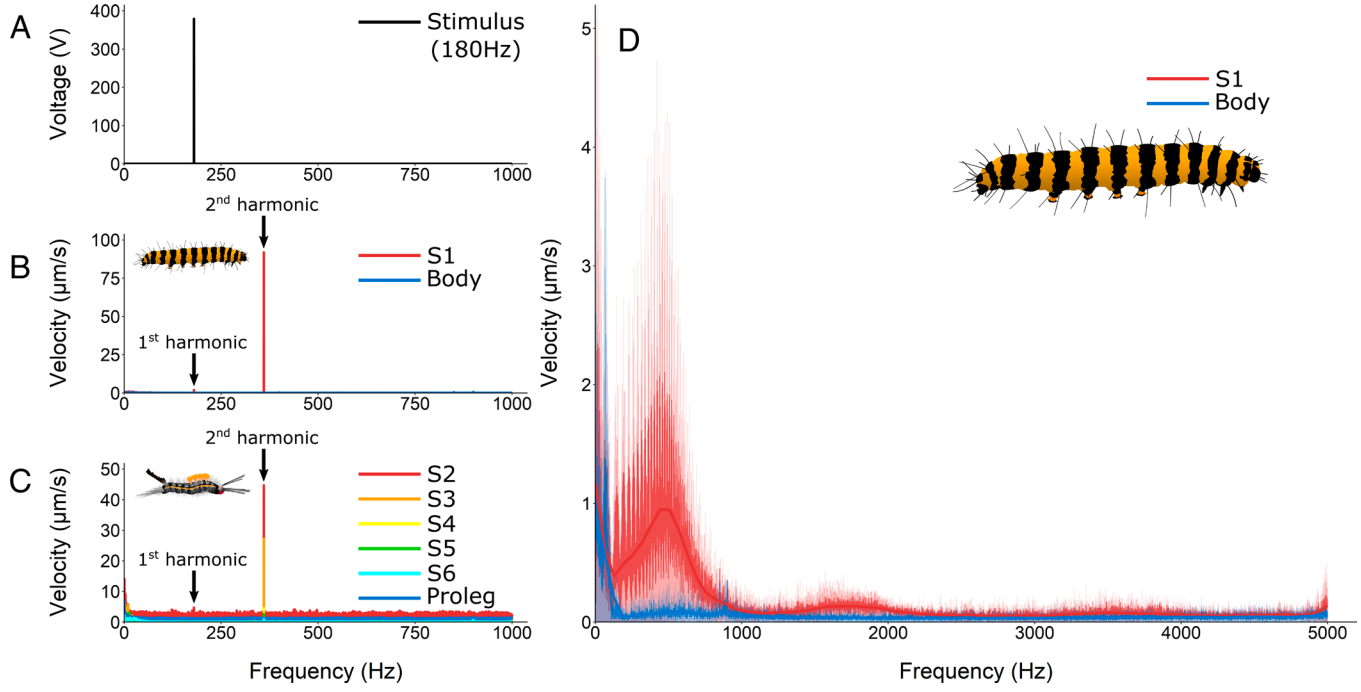

Fig. 5. LDV measurements of the electromechanical response of caterpillar setae to electric field stimuli. (*A*) FFT of the electrical signal supplied to the stimulus delivery system during single frequency trials at 180 Hz (*SI Appendix*, Fig. S3). (*B*) Mean FFT of the electromechanical response of *T. jacobaeae* setae (red, n = 6) and body walls (blue, n = 6) to a 180 Hz electrical stimulus. Maximum response of setae is seen at the 2nd harmonic (360 Hz). (*C*) Mean FFT of the electromechanical response of various types of *T. recens* setae (red, orange, yellow, green, cyan, n = 5 each) and prolegs (blue, n = 5) to a 180 Hz electrical stimulus. (*D*) Mean FFT of the electromechanical response of *T. jacobaeae* setae (red, n = 4) and body walls (blue, n = 4) to a periodic chirp frequency sweep between 0 and 5 kHz. Middle hues show mean FFT of the raw data, lightest hue shows SD of raw data, and darkest hue shows smoothed line of the mean FFT of the raw data, generated using the local regression method with a span of 0.05. Maximum response of setae is seen at 441 Hz.

detect the electric fields around flowers, informing foraging decisions (37, 38). Aerial electroreception has also been shown to be used by honeybees (*Apis mellifera*) when detecting conspecifics performing the waggle dance (39), and in linyphiid spiders detecting the strength of the atmospheric electric fields that provide lift when dispersing by silk ballooning (40, 41). As here with caterpillars, electrostatic actuation of mechanosensory structures has been implicated as the mechanism of detection in these animals (26, 38–40). Due to the ecological and phylogenetic diversity of examples already known, a strong case can be built that aerial electroreception is a widespread sensory modality in terrestrial arthropods. The identification of electroreception in caterpillars substantially bolsters this argument because predator–prey interactions are arguably the most ubiquitous and important ecological interaction in nature, suggesting that a large number of animal species could benefit from aerial electroreception.

One important consequence of the polarization-based mechanism of electroreception revealed for caterpillars here is that caterpillars do not need to possess any net electrical charge of their own to be sensitive to the charge of their predators, akin to how ticks are electrostatically attracted to their hosts irrespective of their own net charge (42). This observation aligns with the finding that caterpillars do not carry a net charge proportionate to their size, as compared with other insects (5). Enticingly, this may allow caterpillars to be electrically camouflaged if any of their predators or parasites use electroreception to locate their prey, while remaining sensitive to electric fields themselves. Thus, an adaptive sensory advantage would be conveyed to the caterpillars during their predator–prey interactions.

Furthermore, while we expect that electroreception can be utilized synergistically with acoustic sensing to improve overall sensitivity via constructive interference, this polarization-based mechanism also allows for electrical and acoustic stimuli to be distinguished from each other despite being sensed by the same sensory structures, an ability predicted previously (15, 27, 40, 43, 44). This may be advantageous if one sensory modality is contextually more reliable than another. However, our experimental evidence presented here, alongside previous theoretical calculations (15, 43, 45, 46), clearly demonstrates that electroreception alone is sufficient to detect the presence, location, and wingbeat, of a charged predator at ecologically useful distances.

Critically, the potential impact of anthropogenic noise on this electrosensory system must be addressed, as many species of caterpillar have already been shown to eat less (47), become stressed (48), and accelerate their development (49) when exposed to sound at the same frequencies tested in this study, all of which result in reduced fitness and survival. This study therefore reveals the possibility that the electrical noise from powerlines and electrical equipment could also have such adverse effects, as well as desensitize caterpillars to genuine predatory cues by sensory habituation or saturation. Exploring this possibility is of even greater urgency in light of recent evidence that anthropogenic activity in the form of synthetic fertilizer application constitutes a source of noise interfering with electroreception in bumblebees (50). We must therefore act swiftly to further characterize the ecological, phylogenetic, and mechanistic breadth of aerial electroreception, as well as human impact upon it, so that mitigation and prevention can be enacted if needed.

Overall, our study reveals that terrestrial animals can utilize electroreception for predator detection. In doing so, it provides further evidence of the ecological importance of naturally occurring electricity, and unveils a dimension of predator–prey interactions ripe for further exploration.

Materials and Methods

Animal Collection and Care. Peacock butterfly caterpillars (*A. io*) and cinnabar moth caterpillars (*T. jacobaeae*) were collected from the wild at various sites around Bristol and Bitton, United Kingdom, and were housed in single species groups in mesh cages (≈30 cm × 30 cm × 30 cm or ≈60 cm × 30 cm × 30 cm), provided with water-potted natural foodplants (stinging nettle, *Urtica dioica*, and ragwort, *Jacobaea vulgaris*, respectively) ad libitum. Scarce vapourer moth caterpillars (*T. recens*) were purchased commercially in their first instar (Worldwide Butterflies Ltd., Dorchester, United Kingdom), and kept in ventilated entomology tubs (height = 14.5 cm, diameter = 11.7 cm), fed ad libitum with oak leaves (*Quercus* spp.). All caterpillar enclosures were kept in electrically shielded, acoustically isolated, and semianechoic rooms to prevent habituation to either electric or acoustic stimuli. Twelve hours of full visible spectrum plus ultraviolet lighting was provided, followed by 12 h of darkness, each 24-h period. Caterpillars of the same species were kept together in identical conditions, regardless of their future inclusion in either treatment or control experimental trials, only being removed from their enclosures immediately prior to involvement in an experiment. After inclusion in any experiment, caterpillars were placed into a different set of enclosures to prevent resampling. All wasps (*V. vulgaris*) were measured in situ at the natural site of their nest in Ashton Court, Bristol, United Kingdom, with a single individual collected as a voucher specimen for confirmation of species identification.

Charge Measurements. The net charges of insects were measured using a modified version of a previously described methodology (11). This method utilizes a picoammeter connected to a shielded ring electrode system. This ring electrode was composed of two concentric conductive rings consisting of copper tape, insulated electrically by a 4 mm thick ring of cardboard between them. The inner ring (diameter = 7.7 cm, width = 2.5 cm) was used as the electrode sensing the signal, while the outer ring (diameter = 8.5 cm, width = 3.1 cm) provided electrical shielding as a reference to ensure that only charges passing through the electrode were measured. The inner ring was connected to the signal-carrying central wire of a coaxial cable, and the outer ring connected to the shielding of the coaxial cable. This cable was wired into a custom-built picoammeter which produced an analog voltage proportional to the current passing through the device. This voltage was then outputted to a data acquisition system (NI USB-6009, National Instruments, Austin, TX), being recorded in MATLAB R2018a (MathWorks, Natick, MA) at 1,000 Hz. As a charged object passes through the ring electrode, a current is electrostatically induced in the inner ring. The trace of this current over time consists of an initial peak, corresponding to the approach of the charged object, and a reflex peak, corresponding to the charged object moving away from the electrode. These two peaks should theoretically be identical to each other but with opposite polarity, and so either can be used for analysis. If the initial peak is chosen, then integrating under that peak with respect to time will yield a value proportional to the net charge carried by the object that passed through the electrode. If the reflex peak is chosen, then integrating under that peak with respect to time will yield a value proportional to the net charge of the object passing through the electrode, but with the opposite sign. Therefore, any values obtained by integration of the reflex peak must by multiplied by negative one, to correct the polarity. In cases where the ambient current was not equal to zero, offsets were applied to the data such that each curve had a baseline of zero, from which the integral could be measured. An example of one of these curves is shown in *SI Appendix*, Fig. S1.

All data files had a notch filter applied to them between 49 and 51 Hz, to reduce the 50 Hz electrical noise stemming from mains electricity. Integrals were obtained using trapezoidal numerical integration in MATLAB. The proportionality between the integral measured by the ring electrode system and the true charge of the object was calibrated by dropping charged pieces of polyurethane foam and polystyrene through the ring electrode system and into a previously calibrated Faraday pail and static monitor system (JCI 147 & JCI 140C, Chilworth Technology Ltd., Southampton, United Kingdom). This yielded a strongly linear relationship (adjusted $R^2 = 0.9898$, $P < 2.2 \times 10^{-16}$), see *SI Appendix*, Fig. S2. Wasps (*V. vulgaris*, n = 612) were measured in situ at their natural nest site in the roots of a fallen tree in a wooded area of Ashton Court, Bristol, United Kingdom, between the 20th and 26th August 2020. The ring electrode was mounted on a tripod and positioned at the entrance of the nest, such that any wasps leaving

or entering the hive would pass through the sensor. Caterpillars (*A. io*, n = 44, *T. jacobaeae*, n = 28, and *T. recens*, n = 38) had their charges measured within the laboratory, inside an electrically shielded room. Because caterpillars could not pass through the ring sensor of their own volition at speed, they needed to be dropped through the sensor manually. Caterpillars were picked up with stainless steel soft entomological forceps. The forceps were electrically grounded immediately prior to picking up each caterpillar, by placing them in contact with a grounded metal table to minimize charge transfer from the forceps to the caterpillars. The handles of the forceps were wrapped in electrically insulating tape, and the operator wore electrically insulating nitrile gloves to eliminate the possibility of electrical potentials being transferred from operator to caterpillar. All caterpillars were measured after having been situated on their hostplants for at least 2 h to ensure that their static charges are representative of those that they accumulate in nature. The temperature and relative humidity were recorded during all charge measurements of wasps and caterpillars.

Computational Modeling. All computational models of the electric fields in nature and the experimental apparatuses were produced using three-dimensional finite element analysis in COMSOL Multiphysics® v. 5.4 (COMSOL AB, Stockholm, Sweden). All models were created using either the Electrostatics or Electric Currents interfaces, as appropriate, within the AC/DC module. The Electrostatics interface requires the relative electric permittivity, ε_r, to be defined for each material, whereas the Electric Currents interface requires both ε_r and the electrical conductivity, σ, to be defined for each material. Complete details of the electrical properties ascribed to each material in the models, along with their sources, can be found in *SI Appendix*, Table S1. All data from the models are presented as two-dimensional slices through the three-dimensional models. Cut lines and points were utilized to extract the electric field strength at precise points and regions of interest. The details specific to each model are included below.

Model of wasp and caterpillar in nature. This model was built within the Electrostatics interface. The model was contained within a 0.2 m × 0.2 m × 0.2 m cube. At the center of this cube, a 0.2 m long cylinder with a diameter of 5 mm was placed, oriented vertically, and bridging the top and bottom surfaces of the cube, representative of the stem of a plant. This cylinder was assigned the material properties of "Plant tissue." Midway up this cylinder, a coarse three-dimensional representation of a generic caterpillar was placed, composed of three intersecting ellipsoids representative of the head, thorax, and abdomen of the caterpillar. In addition, a three-dimensional representation of a wasp, also composed of intersecting ellipsoids and a cone, was constructed based on measurements taken in ImageJ (51) of a scale photograph of *V. vulgaris* collected from the site of the wasp charge measurements. The center of the wasp representation's thorax was positioned approximately 2.23 cm away from the center of the plant stem cylinder, with its height roughly centered on the middle of the caterpillar representation. These two animal representations were both assigned the material properties of "Insect tissue." The remainder of the model was assigned the material properties of "Air." The surface of the wasp representation was assigned a charge of +10 pC, while the surface of the caterpillar representation was assigned a charge of −2 pC, based on the means of the charge measurements made in this study for *V. vulgaris* and *A. io* respectively. The surface of the plant stem cylinder was defined as electrical ground (5, 12, 37, 40, 52, 53).

Model of spherical electrode apparatus for behavioral experiments. This model was built with the use of the Electric Currents interface. The model was contained within a 0.3 m × 0.3 m × 0.3 m cube. At the center of this cube, flush to the bottom surface was placed a 0.2 m × 0.13 m × 0.001 m cuboid, representing the ground plate in the behavioral apparatus. Directly above the center of this cuboid was positioned a sphere with a diameter of 1.5 cm, representing the spherical electrode in the behavioral apparatus. The gap between the surface of the sphere and the surface of the ground plate cuboid was exactly 2.6 cm. The upper side of the sphere had a 1.5 mm minor segment removed from it, and upon the resultant flat surface was attached a 15 cm long cylinder with a diameter of 1 cm, representative of the wooden support in the behavioral apparatus. All the dimensions listed here exactly match those of the components of the behavioral apparatus in real life. The ground plate and spherical electrode representations were assigned the material properties of "Aluminum," the support cylinder representation was assigned the material properties of "Wood," and rest of the domains were assigned the material properties of "Air." The surface of the spherical electrode representation was assigned a voltage of 20 V, derived from the peak voltage of the signal that was supplied to the electrode during behavioral trials. The surface of the ground plate representation, and the bottom surface of the model cube upon which it sat, were defined as electrical ground, as these surfaces were electrically grounded in real life.

Model of parallel plate electrode apparatus for behavioral experiments. This model was built using the Electric Currents interface. The model was contained within a 0.45 m × 0.45 m × 0.45 m cube. At the center of this cube, flush to bottom surface was placed a 0.165 m × 0.1 m × 0.04 m cuboid, representing the silicone rubber block from the behavioral apparatus. Placed directly through the center of this cuboid was a 30 cm long cylinder with a diameter of 3 mm, representative of the bamboo stick penetrating the full depth of the silicone, as in the behavioral apparatus. Either side of this cylinder, centered on its tip, were positioned two identical 0.001 m × 0.1 m × 0.085 m cuboids representing the aluminum plate electrodes. These had a separation of exactly 5.6 cm. Each of these thin cuboids was separately connected on its outer face to another cuboid of dimensions 0.006 m × 0.1 m × 0.085 m, representative of the wooden supports in the behavioral apparatus. All the dimensions listed here were derived from measurements of the actual behavioral apparatus, although the thickness of the aluminum electrode plate representations was slightly increased so that the meshing of the model was not unnecessarily computationally taxing. The silicone block representation was assigned the material properties of "Silicone," the central bamboo stick representation, and the wooden support representations were assigned the material properties of "Wood," and the electrode representations were assigned the material properties of "Aluminum." The remaining domains were assigned the material properties of "Air." The surface of the right-side electrode representation was assigned a voltage of 100 V, as this was the peak voltage of the signal that was supplied to the electrodes during behavioral trials, while the surface of the left-side plate electrode representation and the bottom surface of the entire model was defined as electrical ground.

Model of parallel plate electrode apparatus used for LDV. This model was constructed identically to the previously described parallel plate electrode behavioral apparatus model, but with a few modifications. First, the silicone block and bamboo stick representations were replaced by a 7 cm × 3.1 cm × 1 cm cuboid, at the center of the top surface of which a 10.5 cm cylinder with a diameter of 6 mm was placed, and then atop that cylinder, a 2 cm × 2.5 cm × 1.2 cm cuboid was placed. Together, these structures are representative of the balsa wood platform upon which the caterpillars were placed during LDV measurements. The thin cuboids representing the aluminum plate electrodes also bore different dimensions of 9.5 cm × 9.2 cm × 0.1 cm, as did the thicker cuboids representing the wooden supports, with new dimensions of 9.5 cm × 9.2 cm × 0.6 cm. A horizontal cylindrical hole with a diameter of 8 mm was also made in the left-side cuboids, passing through their thinnest dimensions, to represent the hole drilled in the real-life experimental apparatus. The voltage on the right-side electrode representation was also increased to 380 V, in line with the peak voltage supplied to the electrodes in the LDV experiments.

Behavioral Experiments.

T. jacobaeae and T. recens behavioral experiments. For behavioral experiments on *T. jacobaeae* and *T. recens* caterpillars, their innate reaction to defensively coil when under attack was taken advantage of. In both control and treatment trials, caterpillars were picked up from their host plants with soft entomological forceps and held for 20 s, in order to simulate a physical attack on the caterpillars. This invariably induced a defensive coiling response by the caterpillars (Fig. 1 *A* and *B*). After 20 s, each caterpillar was placed on a grounded aluminum plate directly underneath a 1.5 cm diameter spherical conductive metal electrode held 2.6 cm above the surface of the ground plate. In treatment trials, this electrode was emitting a signal consisting of a 180 Hz sine wave punctuated in 2-s bursts, every 4 s, i.e., 2 s of sine wave, followed by 2 s of electrical silence, repeated indefinitely until the conclusion of the trial. This signal was created by an Agilent 33120a function generator (Agilent Technologies, Inc., Santa Clara, CA) with a peak voltage of 0.5 V, that was then amplified by a custom-built 40× amplifier to a 20 V peak voltage and then outputted to the spherical electrode. This system produced an electric field strength of approximately 310 V/m at the peak voltage in the region to be occupied by the caterpillar (ranging from 300.8 V/m immediately adjacent to the surface of the ground plate to 332.2 V/m at 6 mm above the ground plate, 308.4 V/m at the midpoint) (Fig. 3*A*). Altogether, this signal was intended to coarsely mimic the electric profile of an aerial insect predator hovering in

and out of the vicinity of the caterpillar, as predicted by the measurements and models produced earlier in this study (Fig. 2). In control trials, the signal was generated and amplified in an identical way so that any behaviors arising from the caterpillars detecting noise from the equipment would not confound the results, however, the electrode was disconnected from the amplifier such that there was no electrical signal being emitted from it. In all trials, each caterpillar was filmed at 50 frames per second with a Nikon 3400 DSLR camera equipped with either an F-S DX Micro NIKKOR 85mm f/3.5G ED VR lens or an AF-P DX NIKKOR 18–55mm f/3.5–5.6G lens (Nikon Corporation, Tokyo, Japan). Trials were either alternated between treatment and control conditions (for *T. jacobaeae*) or conducted in an ABBA design (for *T. recens*), and the temperature and relative humidity were recorded in each trial to ensure that environmental and time-related conditions were consistent between the treatment and control groups. After involvement in a trial, caterpillars were placed in a separate enclosure to prevent resampling. Each caterpillar individual was tested only once, being exposed to either treatment conditions or control conditions, but not both. In between each trial, the surface of the ground plate was wiped clean with 70% ethanol and allowed to dry, to reduce the chances of any chemical traces left by a previous caterpillar effecting the behavior of any subsequent caterpillars. Behavioral analysis was applied to the videos resulting from these experiments using BORIS (54), with the person conducting the analysis being blind to whether each caterpillar was in the control or treatment group. For *T. jacobaeae*, it was timed how long from being placed on the ground plate the caterpillar took to uncoil, and also for them to commence walking. Both the time taken to uncoil and the time taken to commence walking are interpreted as proxies for the extent to which each caterpillar believes they are under threat, because both remaining coiled and remaining stationary are behavioral strategies for reducing the risk of attack or detection by predators (16). For *T. recens*, the majority of individuals did not commence walking within a practical timeframe of being placed on the ground plate, and therefore only the time taken to uncoil was assessed for this species. In BORIS, three behavioral states were defined to allow for the calculation of these timings:

"Coiled"–Caterpillar is visibly not contacted by forceps (experimenter has begun moving away if view of caterpillar is temporarily obscured), and is, or was most recently seen to be, curled up with the head contacting posterior sections of the body or pointing in the same direction as the posterior of the animal (within 90 degrees of parallel).

"Uncoiled"–Caterpillar is visibly approximately straight i.e., the caterpillar is not "coiled" (See above).

"Walking"–Caterpillar initiates a movement that results in two or more pairs of abdominal prolegs being lifted and the body showing peristaltic waves as the caterpillar moves forward translationally, not part of the uncoiling process.

The transitions between these behavioral states were defined to a precision of 20 ms, at the frame-by-frame level. The time to uncoil was measured as the total time a caterpillar spent in the "coiled" behavioral state, and the time to commence walking was measured as the total time between a caterpillar entering the "coiled" behavioral state and then subsequently entering the "walking" behavioral state.

***A. io* behavioral experiments.** Because *A. io* caterpillars do not exhibit the same defensive coiling behaviors as *T. jacobaeae* and *T. recens*, a different experimental paradigm was required. For *A. io*, flailing and biting, which are similarly well-known defensive behaviors of caterpillars, were utilized as behavioral proxies for assessing their threat perception instead. To assess any potential influence of predator-mimicking electric fields on these defensive behaviors, an experimental apparatus was assembled consisting of a bamboo stick (length = 30 cm, diameter = 3 mm) pushed into a 4 cm thick block of silicone, such that a 26 cm portion of wooden pole stood stably upright. The top of this pole was positioned such that its tip sat at the midpoint between two parallel plates of aluminum, held 5.6 cm apart by a wooden frame. Each plate measured 10 cm × 8.5 cm. In treatment trials, one of these plates was electrically connected to the same function generator and amplifier system described for the other caterpillar species, producing the same signal, but with a higher peak voltage of 2.5 V (100 V postamplification), while the other plate was connected to electrical ground. This resulted in an electric field strength of approximately 1,850 V/m between the plates (for a horizontal line spanning between the plates, situated 1 cm above the tip of the pole, the minimum electric field strength was 1,735.6 V/m adjacent to the ground plate, the midpoint between the plates was 1,831.2 V/m, and the maximum was 2,019.0 V/m adjacent to the live plate) (Fig. 3*A*). In control trials, the function generator and amplifier were still producing the signal for consistency but were not connected to either of the plates. Instead, both plates were connected to ground so that the electrical signal was not presented to the caterpillars. At the commencement of each trial, a live *A. io* caterpillar was picked up with soft entomology forceps and placed with its legs in contact with the base of the pole, with at least some of its body in contact with the silicone block. Caterpillars were then released from the forceps and allowed to climb the pole, ascending and descending freely, until they remade contact with the silicone, at which point the trial was ended and the caterpillar was removed from the apparatus and placed in a separate enclosure to prevent resampling. To reduce the presence of any chemical traces or cues left by previous caterpillars, the bamboo stick was replaced with a fresh clean stick before each trial, and the plates were wiped clean with 70% ethanol. During their climbing of the pole, caterpillars naturally entered the region between the parallel plates and thus any behavioral responses to the electric stimuli presented between the plates could be assessed. Each individual was only subjected to one trial, either control or treatment. Each trial was filmed at 50 frames per second with a Nikon 3400 DSLR camera equipped with DX NIKKOR 18–55mm f/3.5–5.6G lens (Nikon Corporation, Tokyo, Japan). Trials were alternated between treatment and control conditions and the temperature and relative humidity were recorded to ensure that environmental and time-related conditions were not significantly different between treatment and control groups. Behavioral analysis was performed using BORIS to measure the total amount of time each caterpillar spent flailing, and how many times they bit the electrode. For this, a behavioral state of "flailing" was defined within BORIS. This behavioral state was defined as being from the moment the caterpillar lifted at least one pair of legs away from the pole in a movement that subsequently led to the caterpillar swinging its head and thorax from side to side, to the moment the caterpillar's final pair of legs returned to the pole. A behavioral event of "bite" was also defined in BORIS as when the caterpillar visibly reached out and made contact with one of the electrode plates. These contacts were observed in person to be bites, but due to insufficient spatial resolution on the video recording, individual bites could not be consistently discerned from one another. Instead, each bout of biting was grouped as one "bite," with bouts being deemed separate from one another if the caterpillar visibly moved its head away from the electrode, creating visible space between it and the electrode, before returning to bite again. All behavioral analysis was performed to a frame-by-frame resolution, meaning that the precision of behavioral state transitions was 20 ms. For each caterpillar, the time spent flailing was calculated as the total time it was recorded as being in the "flailing" behavioral state, and the total number of bites was calculated as the sum of all the biting bouts that the caterpillar enacted.

Statistics. All statistical analyses were performed in R 4.2.1 (The R Foundation for Statistical Computing, Vienna, Austria). For all statistical tests, an alpha level of $\alpha = 0.05$ was selected, such that *P*-values less than this threshold would justify rejecting the null hypothesis. Each behavioral dataset was first tested for normality, both visually with Q-Q plots, and statistically with the use of Shapiro–Wilk tests. From these inspections, all the datasets were deemed to possess nonnormal distributions and therefore the Mann–Whitney *U* test, which is a nonparametric test, was selected as the appropriate test for statistical differences in behaviors between the treatment and control groups. Before applying this test, Levene's test was applied to each dataset to test for equality of variances, because the interpretation of the results of Mann–Whitney *U* tests is dependent upon whether the variances are equal between the two sample groups. All but one dataset failed this test for equality of variances, and therefore any statistically significant *P*-values were interpreted to be limited to differences between the mean ranks of the treatment and control groups. It was found that for each of the behaviors tested, significant differences exist between the treatment and control groups, and therefore it is likely that the presence of predator-mimicking electric field induces or modulates defensive behaviors in these species of caterpillar. It is important to note that the data for the number of bites by *A. io* caterpillars contains many ties, and thus the Mann–Whitney *U* test is likely underestimating the statistical significance in this case. Mann–Whitney *U* tests were also applied to the relative humidity and temperature recordings for each dataset, to ensure that differences in environmental conditions were not responsible for the observed differences in behavior. Neither relative humidity nor temperature differed significantly between treatment and control groups within any of the datasets, and therefore the significantly different behavior seen between treatment and control groups

is likely solely due to the electric field stimuli presented to the caterpillars. For details of the results of all the tests, see *SI Appendix*, Table S2.

SEM. Caterpillars intended for imaging by SEM were stored intact, being placed into 70% ethanol for preservation. Prior to imaging, caterpillars were dehydrated further by moving them into 100% ethanol for at least 24 h, and then placing them into a Leica EM CPD300 critical point dryer (Leica Microsystems GmbH, Wetzlar, Germany). After dehydration, caterpillars were sputter coated with conductive metal using an Emitech K757X (Quorum Technologies Ltd., Ashford, United Kingdom). All SEM was performed with the use of an FEI Quanta 200 FEG scanning electron microscope (Field Electron and Ion Company, Hillsboro, Oregon, United States), utilizing a 5.0 kV accelerating voltage and either an Everhart–Thornley detector or a solid-state detector.

LDV. LDV was conducted on two of the caterpillar species: *T. recens* and *T. jacobaeae*. LDV was performed with a Polytec PSV-400 scanning vibrometer, equipped with a Polytec close-up head, PSV-400 Junction box, and controlled with a Polytec OFV-5000 vibrometer controller (Polytec GmbH, Waldbronn, Germany). Measurements were recorded on the Polytec DMS Data Management System running PSV 9.0 acquisition software. The vibrometer range was set to the VD-09 setting (5 mm/s/V), with a fast tracking filter. The fast fourier transform (FFT) measurement mode was used, with complex averaging over 10 samples per measurement, and 6,400 FFT lines. Electrical signals were generated within the software, outputted via the PS4-400 junction box, and then amplified with a custom-built 40× voltage amplifier, connected to two sides of a parallel plate electrode apparatus orientated such that the unperturbed electric field lines would run parallel to the laser beam. This parallel plate electrode apparatus consisted of two aluminum plates attached to a wooden support, holding them 5.6 mm apart. Each plate measured 9.5 cm × 9.2 cm. The sample was placed at the midpoint between these plates, and an 8 mm diameter hole existed at the center of the plate closest to the laser source, through which the laser could reach the sample optically, without any significant perturbation of the electric field (*SI Appendix*, Fig. S3). Black card was adhered to the plate furthest from the laser source to reduce reflections of the laser off this surface, with minimal interference to the electric field. Before measurement, caterpillars were picked up from their host plants with soft entomological forceps, while wearing electrically insulating nitrile rubber gloves so as to keep the animal's electrical charge as close to natural conditions as possible. This action caused the caterpillars to perform a defensive coil as seen in Fig. 1 *A* and *B*, which resulted in them being immobilized for measurement but still being alive. Measurements were performed on live caterpillars so as to eliminate the effect of drying on the mobility of setae. After being picked up and held for long enough to induce coiling, caterpillars were placed atop a balsa wood platform at the center of the parallel plate stimulus delivery system, and measurements were made of candidate electrosensory setae. LDV measurements were also made of the body (for *T. jacobaeae*) or abdominal prolegs (for *T. recens*) to provide a control measurement to ensure that it was the setae, not the whole animal, that was moving in response to the electric field. Control measurements were also taken of the setae but with the capacitor plate disconnected from the amplifier such that any movements of the setae could be verified as being a result of the applied electrical stimulus. Two stimuli were presented to the caterpillars separately; a single frequency sine wave at 180 Hz to verify an electromechanical response to the specific frequency used in the behavioral experiments, and a periodic chirp between 0 and 5,000 Hz to search for any potential electromechanical resonances of the setae. Each of these stimuli had a peak voltage from the signal generator of 9.5 V, amplified to 380 V by the amplifier. This produced an electric field strength of approximately 7.88 kV/m modeled at the midpoint between the electrode plates (*SI Appendix*, Fig. S3*B*). For *T. jacobaeae*, the conspicuous primary setae distributed across the body were investigated. For *T. recens*, five different seta types were investigated due to their morphological diversity (Fig. 4). Single point measurements were taken per seta per animal (e.g., *SI Appendix*, Fig. S3*C*. See also Fig. 5 for the number of individuals i.e., sample sizes). All measurements took place on an antivibration table situated in an acoustically isolated, semianechoic, and electrically shielded room.

Data, Materials, and Software Availability. Behavioural data, charge data, and LDV data have been deposited in Mendeley Data (55) (https://doi.org/10.17632/t37j65bd6m.1).

ACKNOWLEDGMENTS. We would like to thank Talia Sullens for her help in collecting and raising the caterpillars and providing feedback on an early draft of the manuscript; Katie Lihou, Benito Wainwright, Luke Romaine, Duncan Edgley, and Toby Champneys for their help collecting caterpillars; Judith Mantell for her assistance with the electron microscopy; Kosta Manser for creating the insect iconography; and Liam O'Reilly, Benito Wainwright, Fraser Woodburn, Tom Neil, Eleine Gomez, and Chantal Mears for their feedback on the manuscript.

1. C. Darwin, *On the Origin of Species by Means of Natural Selection, or Preservation of Favoured Races in the Struggle for Life* (John Murray, 1859).
2. R. Dawkins, J. R. Krebs, Arms races between and within species. *Proc. R. Soc. London Ser. B. Biol. Sci.* **205**, 489–511 (1979).
3. R. T. Paine, Food web complexity and species diversity. *Am. Nat.* **100**, 65–75 (1966).
4. C. Coulomb, *Premier mémoire sur l'électricité et le magnétisme* (Histoire de l'Académie Royale des Sciences, 1785).
5. S. J. England, D. Robert, The ecology of electricity and electroreception. *Biol. Rev.* **97**, 383–413 (2022).
6. E. R. Hunting *et al.*, Challenges in coupling atmospheric electricity with biological systems. *Int. J. Biometeorol.* **65**, 45–58 (2021).
7. D. K. Edwards, A method for continuous determination of displacement activity in a group of flying insects. *Can. J. Zool.* **38**, 1021–1025 (1960).
8. D. K. Edwards, Laboratory determinations of the daily flight times of seperate sexes of some moths in naturally changing light. *Can. J. Zool.* **40**, 511–530 (1962).
9. E. H. Erickson, Surface electric potentials on worker honeybees leaving and entering the hive. *J. Apic. Res.* **14**, 141–147 (1975).
10. S. Gan-Mor, Y. Schwartz, A. Bechar, D. Eisikowitch, G. Manor, Relevance of electrostatic forces in natural and artificial pollination. *Can. Agric. Eng.* **37**, 189–194 (1995).
11. C. Montgomery, K. Koh, D. Robert, Measurement of electric charges on foraging bumblebees (*Bombus terrestris*). *J. Phys.: Conf. Ser.* **1322**, 012002 (2019).
12. E. R. Hunting *et al.*, Observed electric charge of insect swarms and their contribution to atmospheric electricity. *iScience* **25**, 105241 (2022).
13. O. Sotavalta, "The flight-sounds of insects" in *Acoustic Behaviour of Animals*, R.-G. Busnel, Ed. (Elsevier, 1963), pp. 374–390.
14. A. Rashed, M. I. Khan, J. W. Dawson, J. E. Yack, T. N. Sherratt, Do hoverflies (Diptera: Syrphidae) sound like the Hymenoptera they morphologically resemble? *Behav. Ecol.* **20**, 396–402 (2009).
15. R. A. Palmer, L. J. O'Reilly, J. Carpenter, I. V. Chenchiah, D. Robert, An analysis of time-varying dynamics in electrically sensitive arthropod hairs to understand real-world electrical sensing. *J. R. Soc. Interface* **20**, 20230177 (2023).
16. H. F. Greeney, L. A. Dyer, A. M. Smilanich, Feeding by lepidopteran larvae is dangerous: A review of caterpillars' chemical, physiological, morphological, and behavioral defenses against natural enemies. *Invertebr. Surviv. J.* **9**, 7–34 (2012).
17. H. Markl, J. Tautz, The sensitivity of hair receptors in caterpillars of *Barathra brassicae* L. (Lepidoptera, Noctuidae) to particle movement in a sound field. *J. Comp. Physiol. A* **99**, 79–87 (1975).
18. C. P. B. Breviglieri, G. Q. Romero, Acoustic stimuli from predators trigger behavioural responses in aggregate caterpillars. *Austral Ecol.* **44**, 880–890 (2019).
19. J. Tautz, H. Markl, Caterpillars detect flying wasps by hairs sensitive to airborne vibration. *Behav. Ecol. Sociobiol.* **4**, 101–110 (1978).
20. C. J. Taylor, J. E. Yack, Hearing in caterpillars of the monarch butterfly (*Danaus plexippus*). *J. Exp. Biol.* **222**, jeb211862 (2019).
21. D. E. Minnich, The responses of caterpillars to sounds. *J. Exp. Zool.* **72**, 439–453 (1936).
22. M. Rothschild, G. Bergström, The monarch butterfly caterpillar (*Danaus plexippus*) waves at passing hymenoptera and jet aircraft – Are repellent volatiles released simultaneously? *Phytochemistry* **45**, 1139–1144 (1997).
23. T. R. White, J. S. Weaver, H. R. Agee, Response of *Cerura borealis* (Lepidoptera: Notodontidae) larvae to low-frequency sound. *Ann. Entomol. Soc. Am.* **76**, 1–5 (1983).
24. D. E. Minnich, The reactions of the larvae of *Vanessa antiopa* Linn. to sounds. *J. Exp. Zool.* **42**, 443–469 (1925).
25. J. H. Myers, J. N. M. Smith, Head flicking by tent caterpillars: A defensive response to parasite sounds. *Can. J. Zool.* **56**, 1628–1631 (1978).
26. G. P. Sutton, D. Clarke, E. L. Morley, D. Robert, Mechanosensory hairs in bumblebees (*Bombus terrestris*) detect weak electric fields. *Proc. Natl. Acad. Sci. U.S.A.* **113**, 7261–7265 (2016).
27. K. Koh *et al.*, Bumblebee hair motion in electric fields. *J. Phys.: Conf. Ser.* **1322**, 012001 (2019).
28. D. N. Byrne, S. L. Buchmann, H. G. Spangler, Relationship between wing loading, wingbeat frequency and body mass in homopterous insects. *J. Exp. Biol.* **135**, 9–23 (1988).
29. M. A. B. Deakin, Formulae for insect wingbeat frequency. *J. Insect Sci.* **10**, 96 (2010).
30. N. S. Ha, Q. T. Truong, N. S. Goo, H. C. Park, Relationship between wingbeat frequency and resonant frequency of the wing in insects. *Bioinspir. Biomim.* **8**, 046008 (2013).
31. A. J. Kalmijn, Electro-perception in sharks and rays. *Nature* **212**, 1232–1233 (1966).
32. A. J. Kalmijn, The electric sense of sharks and rays. *J. Exp. Biol.* **55**, 371–383 (1971).
33. R. M. Kempster, I. D. McCarthy, S. P. Collin, Phylogenetic and ecological factors influencing the number and distribution of electroreceptors in elasmobranchs. *J. Fish Biol.* **80**, 2055–2088 (2012).
34. R. M. Kempster, N. S. Hart, S. P. Collin, Survival of the stillest: Predator avoidance in shark embryos. *PLoS One* **8**, e52551 (2013).
35. W. G. R. Crampton, Electroreception, electrogenesis and electric signal evolution. *J. Fish Biol.* **95**, 92–134 (2019).
36. A. Y. Kawahara *et al.*, Phylogenomics reveals the evolutionary timing and pattern of butterflies and moths. *Proc. Natl. Acad. Sci. U.S.A.* **116**, 22657–22663 (2019).
37. D. Clarke, H. Whitney, G. Sutton, D. Robert, Detection and learning of floral electric fields by bumblebees. *Science.* **340**, 66–69 (2013).
38. S. A. Khan *et al.*, Electric field detection as floral cue in hoverfly pollination. *Sci. Rep.* **11**, 1–9 (2021).

39. U. Greggers *et al.*, Reception and learning of electric fields in bees. *Proc. R. Soc. B Biol. Sci.* **280**, 20130528 (2013).
40. E. L. Morley, D. Robert, Electric fields elicit ballooning in spiders. *Curr. Biol.* **28**, 2324–2330.e2 (2018).
41. N. Narimanov, D. Bonte, P. Mason, L. Mestre, M. H. Entling, Disentangling the roles of electric fields and wind in spider dispersal experiments. *J. Arachnol.* **49**, 380–383 (2021).
42. S. J. England, K. Lihou, D. Robert, Static electricity passively attracts ticks onto hosts. *Curr. Biol.* **33**, 3041–3047.e4 (2023).
43. R. A. Palmer, I. V. Chenchiah, D. Robert, Analysis of aerodynamic and electrostatic sensing in mechanoreceptor arthropod hairs. *J. Theor. Biol.* **530**, 110871 (2021).
44. K. Koh, D. Robert, Bumblebee hairs as electric and air motion sensors: Theoretical analysis of an isolated hair. *J. R. Soc. Interface* **17**, 20200146 (2020).
45. R. A. Palmer, I. V. Chenschiah, D. Robert, The mechanics and interactions of electrically sensitive mechanoreceptive hair arrays of arthropods. *J. R. Soc. Interface* **19**, 20220053 (2022).
46. R. A. Palmer, I. V. Chenchiah, D. Robert, Passive electrolocation in terrestrial arthropods: Theoretical modelling of location detection. *J. Theor. Biol.* **558**, 111357 (2023).
47. J. Tautz, M. Rostás, Honeybee buzz attenuates plant damage by caterpillars. *Curr. Biol.* **18**, R1125–R1126 (2008).
48. A. K. Davis, H. Schroeder, I. Yeager, J. Pearce, Effects of simulated highway noise on heart rates of larval monarch butterflies, *Danaus plexippus*: Implications for roadside habitat suitability. *Biol. Lett.* **14**, 20180018 (2018).
49. Z. A. Lee, A. K. Baranowski, E. L. Preisser, Auditory predator cues affect monarch (*Danaus plexippus*; Lepidoptera: Nymphalidae) development time and pupal weight. *Acta Oecol.* **111**, 103740 (2021).
50. E. R. Hunting *et al.*, Synthetic fertilizers alter floral biophysical cues and bumblebee foraging behavior. *PNAS Nexus* **1**, pgac230 (2022).
51. C. A. Schneider, W. S. Rasband, K. W. Eliceiri, NIH Image to ImageJ: 25 years of image analysis. *Nat. Methods* **9**, 671–675 (2012).
52. D. Clarke, E. Morley, D. Robert, The bee, the flower, and the electric field: Electric ecology and aerial electroreception. *J. Comp. Physiol. A Neuroethol. Sensory Neural Behav. Physiol.* **203**, 737–748 (2017).
53. E. R. Hunting, S. J. England, D. Robert, Tree canopies influence ground level atmospheric electrical and biogeochemical variability. *Front. Earth Sci.* **9**, 562 (2021).
54. O. Friard, M. Gamba, BORIS: A free, versatile open-source event-logging software for video/audio coding and live observations. *Methods Ecol. Evol.* **7**, 1325–1330 (2016).
55. S. J. England, D. Robert, Data from "Prey can detect predators via electroreception in air – data", Mendeley Data. Available at https://doi.org/10.17632/t37j65bd6m.1. Deposited 29 April 2024.